Sādhanā Vol. 38, Part 6, December 2013, pp. 1347–1356. © Indian Academy of Sciences

Cold test of cylindrical open resonator for 42 GHz, 200 kW gyrotron

VIVEK YADAV[1,2,*], SUDEEP SHARAN[1], HASINA KHATUN[1], NITIN KUMAR[1], M K ALARIA[1], B JHA[3], S C DEORANI[2], A K SINHA[1] and P K JAIN[3]

[1]Gyrotron Laboratory, MWT Area, Central Electronics Engineering Research Institute (A constituent Laboratory of Council of Scientific and Industrial Research), Pilani 333 031, India
[2]Department of Physics, R R College, University of Rajasthan, Alwar 301 001, India
[3]Centre for Research in Microwave Tubes (CRMT), Banaras Hindu University, Varanasi 221 005, India
e-mail: vivek.ceeri08@gmail.com

MS received 4 July 2011; accepted 1 June 2013

Abstract. This paper presents experimental results for cold testing of a gyrotron open resonator. Experiments were carried out to measure resonant frequency and their particular quality factor for TE mode at the frequency 42 GHz. The perturbation technique was used to determine the axial, radial and azimuthal electric field profile for identification of TE_{031} mode at operating frequency 42 GHz. The good agreement between experimental results and theoretical studies was found. The results verify the design and fabrication of the specific gyrotron cavity.

Keywords. Gyrotron; resonator; electric field profile; perturbation technique.

1. Introduction

Gyrotron is a high power, high frequency millimeter wave source which generates coherent electromagnetic radiation. The device is used in plasma fusion, material processing, NMR spectroscopy and millimeter wave radar system (Thumm 2005). Recently in India, a program of design and development of the 42 GHz, 200 kW gyrotron has been initiated for the Indian TOKAMAK system. The basic specifications of the gyrotron are shown in table 1. The power growth in the gyrotron occurs inside the specially designed RF resonator. The gyrating electron beam, generated from the Magnetron Injection Gun, interacts with a particular TE mode in the resonator and transfer an amount of its perpendicular kinetic energy to the RF. The output power, the output frequency and the interaction efficiency of the gyrotron critically depend on the eigenfrequency, Q value and the mode excitation in the resonator (Kartikeyan *et al* 2004; Flyagin *et al*

*For correspondence

Table 1. Basic specifications of 42 GHz gyrotron.

Operating mode	TE_{03}
Operating frequency (f_0)	42 GHz
Beam voltage (V_0)	65 kV
Beam current (I_0)	10 A
Output power (P_0)	200 kW
Efficiency (η)	33%

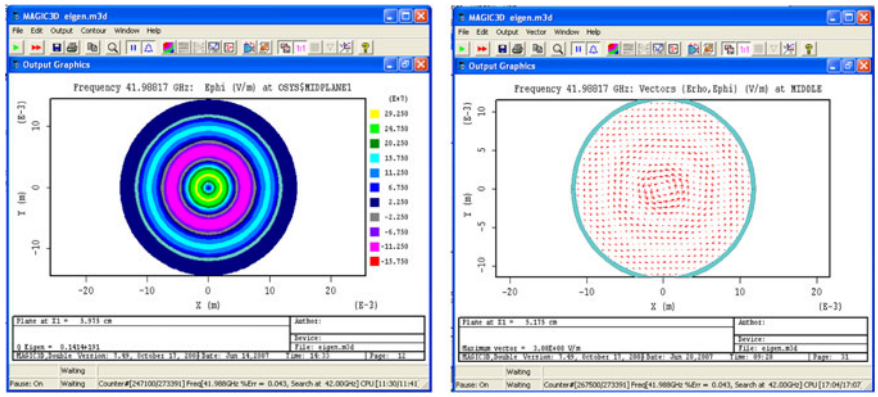

Figure 1. Contour and vector plot of electric field at the cross sectional top view of tapered cavity for TE_{031} mode. (**a**) Contour plot. (**b**) Vector plot.

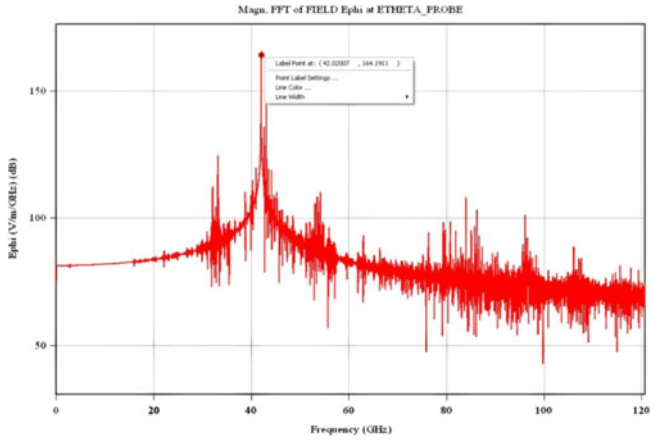

Figure 2. Frequency spectrum of the electric field (Beam current 10 A, Beam voltage 65 kV, Magnetic field 1.61 T).

1977; Thumm 2007). The cold characterization of the gyrotron resonator has been considered to see its performance before the final assembly of the device.

This paper presents the experimental results of the cold testing of the 42 GHz gyrotron resonator. It focuses on the TE_{031} mode between other fundamental modes at operating frequency. The axial, radial and azimuthal electric field profile has also been determined to identify the excited mode. The experimental results has also been compared with the numerically simulated results obtained from the MAGIC simulation tool as shown in figures 1 and 2. The operating parameters used in MAGIC are given in figure 2. For the cold testing of the gyrotron resonator, perturbation techniques have been used (Barroso *et al* 1997; Castro *et al* 2000). The resonance frequency has been determined by the transmission technique and the loaded quality factor has been commuted by half power bandwidth method at −3 dB point. The standing wave electric field profile has been determined by moving a dielectric object of $\lambda/10$-diameter in axial, radial and azimuthal directions.

2. Gyrotron resonator

The interaction resonator for most gyrotrons consists of a simple cylinder with a down taper at the entrance and up taper at the cavity exit (Kartikeyan *et al* 2004). The input taper is a cut-off section, which prevents the back propagation of RF power to the gun. The beam wave interaction takes place mainly in the uniform middle section where the RF field reaches the peak value. The up taper connects the cavity with output waveguide and the quasi-optical launcher. The junction between the sections is made smooth in order to minimize unwanted mode conversion at sharp edges. The up and down taper of the cavity provide enough reflection to maintain a standing wave field in the cavity. Reflections at the tapers lead to resonant behaviour of the cavity (Kartikeyan *et al* 2004; Flyagin *et al* 1977; Thumm 2007). Figure 3 shows the resonator geometry for the 42 GHz gyrotron.

For the single mode estimation, the longitudinal distribution of electric field satisfies the wave equation (Vlasov *et al* 1969):

$$\frac{d^2V(z)}{dz^2} + K_{II}^2(z)V(z) = 0. \tag{1}$$

Subject to appropriate radiation conditions at cavity ends:

$$\frac{dV(z)}{dz} \mp iK_{II}V(z)\Big|\, z_{in}, z_{out} = 0, \tag{2}$$

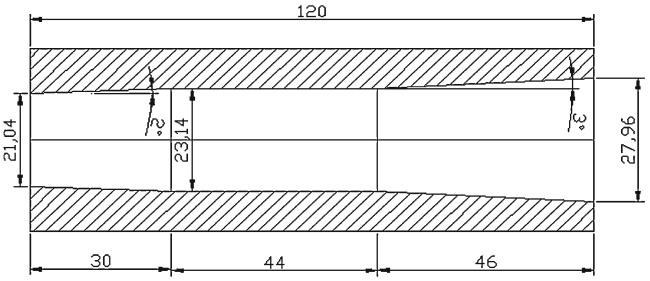

Figure 3. Cut way view of gyrotron cavity (all dimensions are in mm).

where $K_{II,mp} = \left(\omega/c^2 - K_{\perp,mp}^2\right)^{1/2}$ is the longitudinal wave number and $K_{\perp,mp}$ is the transverse wave number with m and p denoting the azimuthal and radial indices. The resonator Q factor measured here is the total or loaded Q as determined by the ratio of the measured resonance line width at half maximum to the absolute resonance frequency. It is related to the diffractive and ohmic Q by (Woskoboinikow and Mulligan 1987)

$$Q_T = \left(Q_D^{-1} + Q_\Omega^{-1}\right)^{-1}. \tag{3}$$

The diffractive Q describes the balance between the energy stored in the cavity E_S and the output coupled power P. For gyrotron cavity it can be defined as (Barroso *et al* 1997)

$$Q_D = \frac{4\pi}{(1 - R_1 R_2)} \left[\frac{L}{\lambda}\right]^2, \tag{4}$$

where R_1 and R_2 are reflectivities at the ends of the cavity and L is the axial length of the stored field.

The ohmic Q describes the balance between the energy stored in the cavity and the power coupled to the cavity wall. For gyrotron cavity it can be defined as (Woskoboinikow and Mulligan 1987)

$$Q_\Omega = \frac{R_0}{\delta}\left(1 - \frac{m^2}{\gamma_{mp}^2}\right), \tag{5}$$

where R_0 is the cavity radius, δ is the skin depth, γ_{mp} is the pth zero of the J_m' Bessel function.

3. Experimental

In this method, an electric probe is inserted through 1 mm diameter hole at the center of the middle section of the cavity for the excitation of TE mode. A pyramidal horn antenna is used as a receiver in the far field region. Vector Network Analyzer (VNA) is used as a RF source. Figure 4 shows the experimental set-up for the measurement of eigenfrequency (f) and the total quality factor (Q_T). The eigenfrequency is measured by the resonance curve displayed on the VNA display. The loaded quality factor is calculated by half power bandwidth method at -3 dB point.

The standing electric field profile is measured by using the perturbation technique (Castro *et al* 2000). A dielectric object is used for the perturbation of electric field inside the cavity. The electric field intensity is measured by the shift in resonance frequency, according to Slater–Tisher theorem as shown in the following expression (Tisher 1963; Ginzton 1957):

$$\frac{f - f_0}{f_0} = \frac{\Delta W_E - \Delta W_H}{W_E - W_H}, \tag{6}$$

where W_E, W_H, ΔW_E and ΔW_H are the maximum electric energy, maximum magnetic energy, change in the electric and magnetic energies, respectively.

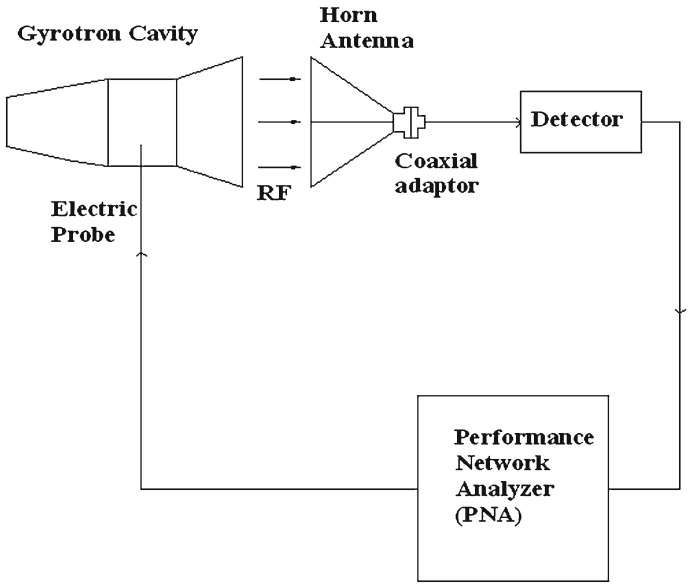

Figure 4. The experimental set-up for the measurement of eigenfrequency and the total quality factor.

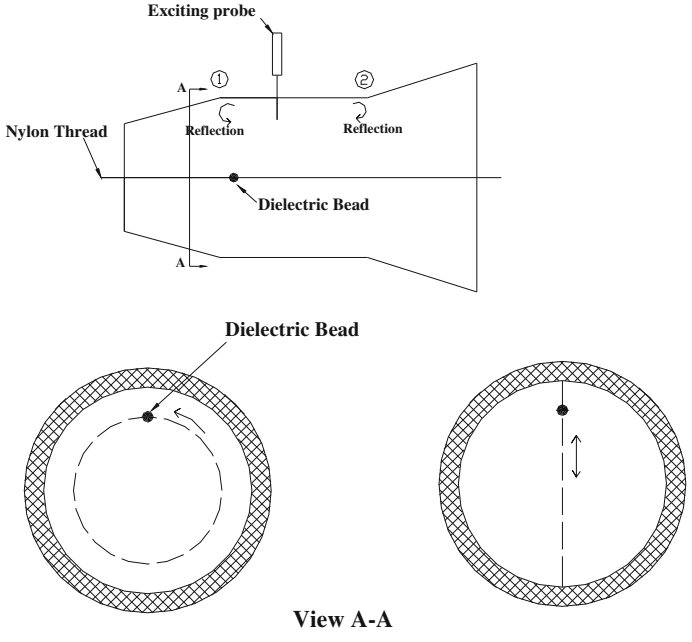

Figure 5. Experimental arrangement for measuring the electric field profile.

For a small spherical dielectric bead of radius a, the change in the electric field energy ΔW_E is negligible i.e., the electric field intensity directly depends on the shift in resonance frequency as shown in the following equation (Tisher 1963; Ginzton 1957):

$$\frac{\Delta f}{f_0} = \pi a^3 \varepsilon_0 \frac{\varepsilon - \varepsilon_0}{\varepsilon + 2} \frac{E^2(z)}{\Delta W_E}, \tag{7}$$

where, ε is the permittivity of the dielectric object.

The axial, radial and azimuthal electric field profile are measured by moving the dielectric object in the axial, radial and azimuthal directions, respectively as shown in figure 5. The nylon thread of 0.5 mm diameter is used to move the dielectric object inside the cavity.

4. Results and discussions

The resonator is manufactured by brass and the dimensions of the resonator are measured after fabrication. The maximum tolerance in the dimensions is ± 0.1 mm. In this sense, we can verify that the results are reliable, within the limits of experimental errors. The surface roughness of the resonator is few microns according to Scanning Electron Microscopy (SEM) image as shown in figure 6. According to eq. (3), the total quality factor Q_T of the fundamental TE mode, is dominated by diffractive rather than wall loss, because Q_D is much smaller than $Q_\Omega (Q_\Omega > 16000)$ (Nusinovich 2004; Edgcombe 1993; Choi 2007). The loaded quality factor is determined by the transmission technique using half power bandwidth method at -3 dB point. For the gyrotron resonator, both types of methods i.e., transmission and reflection, can be used. Due to the tapered section on both side of the middle section, standing wave formation takes place in the middle section. The output taper section angle is determined in such a way that a fraction of the RF can propagate through it and the rest of fraction get reflected towards middle section for the standing wave formation, which is essential for the beam-wave interaction. Due to the resonance in middle section, -3 dB resonance depth is very obvious in the measurements. Finally, the

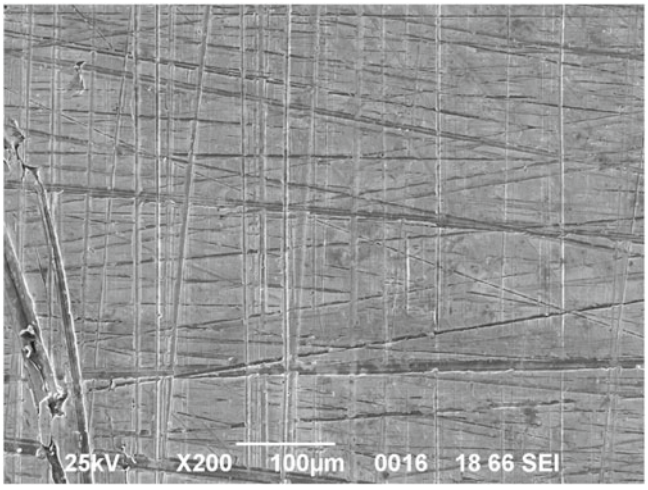

Figure 6. Surface image of the resonator obtained from SEM.

matching of the experimental value of Q factor with the theoretical values also confirm the method.

The loaded Q depends on the output taper angle, input taper angle and the sharpness of the edges. In the fabrication of resonator, the joints between the middle section and tapered sections are made parabolic to avoid the unwanted reflections (Kartikeyan 2008). Due to some fabrication limitations, the edges are not parabolic (sharp edges) in the measured resonator, which raise more reflection towards the middle section. More reflection towards the middle section means more resonance which again indicates high Q. This is the main reason of higher measured Q compared to calculated Q.

To identify the mode of interest, TE_{031}, its standing wave electric field profile in the axial, radial and azimuthal directions were measured by perturbation technique. For this purpose, 1 mm diameter Teflon sphere is used to detect the perturbation in frequency without affecting the total quality factor Q_T.

Figure 7 shows the resonance curve used to calculate the loaded Q and frequency of the resonator. Comparison of calculated and measured resonant frequency and loaded Q (Q_T) factor is presented in table 2. A good agreement is found between measured and calculated values.

Figure 8 shows the comparison between the measured points of axial electric field profile and the theoretical axial electric field profile. Several measurements were done to determine these data of axial electric field profile. So, a realistic agreement is obtained in all these measurements.

Figure 9 shows the comparison between the measured points of radial electric field profile and the theoretical radial electric field profile. In this case, the axial distance of the sphere remained

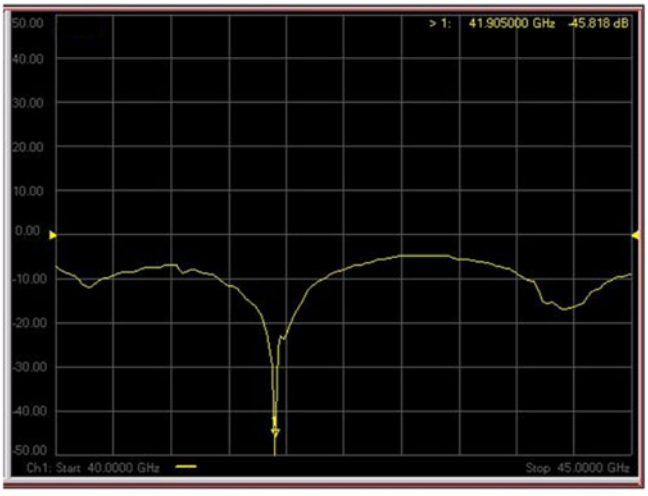

Figure 7. Resonance curve of the resonator.

Table 2. Calculated and measured values of eigenfrequency and quality factor for TE modes.

	Calculated	Measured	Calculated			Measured
	f (GHz)	f (GHz)	Q_D	Q_Ω	Q_T	Q_T
TE_{031} mode	41.9889	41.91	889	25461	860	910

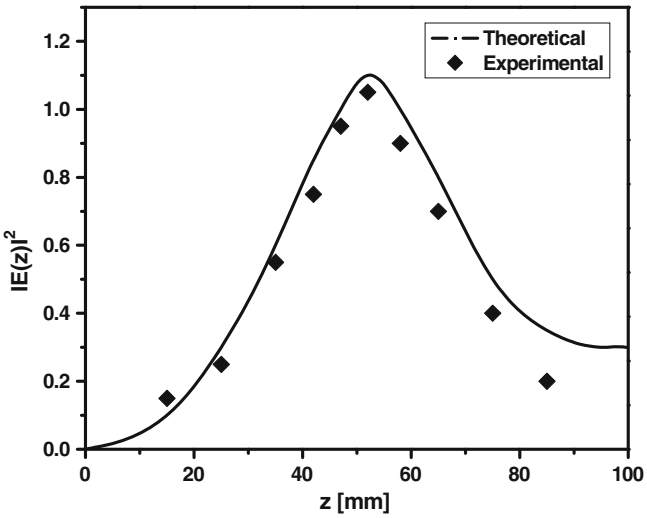

Figure 8. Axial electric field profile for TE_{031} mode.

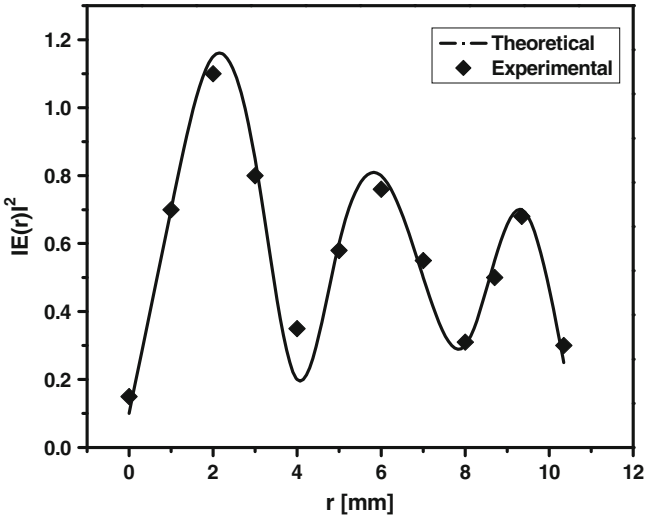

Figure 9. Radial electric field profile for TE_{031} mode.

same and the displacement was in radial direction. So the agreement between measurements and theory is excellent.

Figure 10 shows the measured points of azimuthal electric field profile. In figure 10, it seems that no variation in electric field profile in azimuthal direction, which is expected theoretically. In this measurement the sphere moved azimuthally at the position of maximum intensity of the electric field.

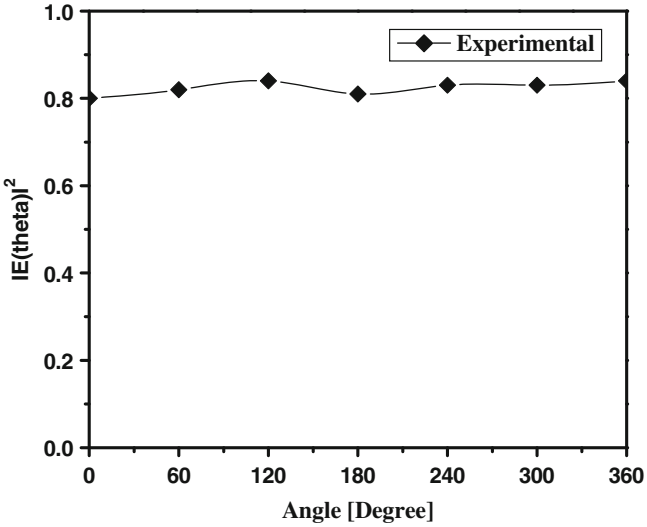

Figure 10. Azimuthal electric field profile for TE_{031} mode.

In figures 8, 9 and 10, the electric field profiles indicate the variation in electric field in axial, radial and azimuthal direction. So the measured axial, radial and azimuthal electric profile shows q = 1, p = 3 and m = 0, respectively for the TE_{031} mode. The nearest strongest competing modes of TE_{031} mode are TE_{231} (resonant frequency 41.16 GHz) and TE_{521} (resonant frequency 43.49 GHz) and the theoretical values of total quality factor Q_T of these modes are 1033 and 500, respectively. So according to results shown in table 2, we can conclude that the TE_{031} mode is likely to be excited due to the frequency separation between the nearest competitors (TE_{231} and TE_{521}). The measurements clearly indicate the excitation of TE_{03} mode at 42 GHz frequency which again verify the design and fabrication of the resonator.

5. Conclusion

An open resonator for 42 GHz gyrotron is fabricated by brass and experimentally studied. Experiments are accomplished to measure resonant frequency and their particular quality factor for TE mode at the frequency 42 GHz. The axial, radial and azimuthal electric field profile were also determined for identification of TE_{031} mode. The good agreement between experimental and theoretical work was found. The results verify the design and fabrication of the specific gyrotron cavity.

Acknowledgements

Authors are thankful to the Director, Central Electronics Engineering Research Institute (CEERI), Pilani, for permission to publish this paper. Thanks are due to Dr. S N Joshi, Dr. V Srivastava, Dr. R S Raju and Team Members for their continuous support and encouragement. Authors are also thankful to Dr L M Joshi and Devashish Pal of Klystron Group, CEERI, Pilani

for providing the PNA facility. Authors are also thankful to Dr. K Rangra for support in experiments. Authors are also thankful to the Department of Science and Technology (DST), New Delhi for funding this project.

References

Barroso J J, Castro P J, Pimenta A A, Spassov V A, Correa R A, Idehara T and Ogawa I 1997 *International Journal of Infrared and Millimeter Waves* 18(11): 611–616, pp. 2147–2160

Choi E 2007 PhD Thesis, MIT USA, pp. 57

Castro P J, Barroso J J and Correa R A 2000 *International Journal of Infrared and Millimeter Waves* 21(4): 633–645

Castro P J, Barroso J J and CorrCa R A 0000 *SBMO/IEEE M'IT-S IMOC'99 Proceedings*

Edgcombe C J (ed) 1993 London: Taylor & Francis

Flyagin V A, Gaponov A V, Petelin I and Yulpatov V K 1977 *IEEE Trans. Microwave Theory Techniques* 25(6): 514–521

Ginzton E L 1957 *Microwave Measurements*, New York: McGraw Hill

Kartikeyan M V 2008 *IEEE Transactions on Plasma Sciences* 36(3)

Kartikeyan M V, Borie E and Thumm M K A 2004 *Gyrotron: high power microwave and millimetre wave technology*, Springer

Nusinovich G S 2004 Maryland: JHU, USA

Singh R K and Jain P K 2008 *International Journal of Electrical and Electronics Engineering* 2:3, 204

Thumm M 2005 *Int. J. Infrared Millim. Waves* 26: 483–503

Thumm M 2007 Forschungszentrum Karlsruhe, Karlsruhe, Germany, Scientific Report FZKA 7289

Tisher F 1963 Izd. Fiz.-Mat. Moscow, Russia: Literatury, pp. 333–347

Vlasov S N, Zhislin G M, Orlova I M, Petelin M I and Rogacheva G G 1969 *Radiophysics and Quantum Electronics* 12(8): 972–978

Woskoboinikow P P and Mulligan W J 1987 *IEEE Transactions on Microwave Theory and Techniques*, mtt-35(2)